Eulerian Network Model of Air Traffic Flow in Congested Areas†

Alexandre M. Bayen♯ Robin L. Raffard♭ Claire J. Tomlin♮

***Abstract*— We derive an Eulerian network model applicable to air traffic flow in the National Airspace System. The model relies on a modified version of the Lighthill-Whitham-Richards (LWR) partial differential equation (PDE), which contains a velocity control term inside the divergence operator. We relate the PDE to aircraft count, which is a key metric in Air Traffic Control. Using the method of characteristics, we construct an analytical solution to the LWR PDE for the case in which the control depends only on space (and not time). We validate our model against real Air Traffic Data (ETMS data), by first showing that the Eulerian description enables good aircraft count predictions, provided a good choice of numerical parameters is made. Finally, we show some predictive capabilities of the model.**

I. INTRODUCTION

There is no single component which defines the *National Airspace System* (NAS), but rather a multitude of systems including aircraft, control facilities, procedures, navigation and surveillance equipment, analysis equipment, as well as the humans (controllers, pilots) who operate the systems. In this paper, we are interested in the *Traffic Flow Management* (TFM), which is a unit whose goal is to try to optimize the flow. This entails preventing the density of aircraft from becoming too large in certain regions of airspace, and operating efficient reroutes when the weather does not allow traffic to cross a given region of airspace. These tasks are currently not optimized with respect to throughput or maximal density tolerable for Air Traffic Controller efficiency. Rather, they are prescribed by *playbooks*, which are procedures that have been established over time, based on Controller experience.

The goal of this article and the companion paper [2] is to derive a model for this system, and a mathematical method to create an optimization strategy capable of automatically generating more efficient control strategies for these tasks. We are interested in deriving "flow patterns", that is, coming up with ways to route streams of aircraft by generating the corresponding aircraft velocities. The individual identity of the aircraft is thus not important, since the objective of such tasks is to come up with a more efficient use of the airspace, rather than optimizing local trajectories of aircraft.

† Research supported by NASA under Grant NCC 2-5422, by ONR under MURI contract N00014-02-1-0720, by DARPA under the Software Enabled Control Program (AFRL contract F33615-99-C-3014), and by a Graduate Fellowship of the Délégation Générale pour l'Armement (France).

♯ IEEE Member, Major (Ingénieur Principal de l'Armement), DGA, France. Autonomous Navigation Laboratory, LRBA, Vernon, France. Corresponding author. bayen@stanford.edu. Tel: (33-2)-27.24.41.87, Fax: (33-2)-27.24.44.99

♭ Ph.D. Student, Aeronautics and Astronautics, Stanford University.

♮ Assistant Professor, Aeronautics and Astronautics, Courtesy Assistant Professor, Electrical Engineering; Director, Hybrid Systems Laboratory, Stanford University.

Ideally, one would like to automatically generate Air Traffic Control - friendly procedures of the following kind: "aircraft on airway 148 at 33,000 ft, fly at 450 kts for the next hour and then accelerate by 25 kts for the next half hour". This suggests following an *Eulerian* approach advocated by Menon et al. [10] and dividing the airspace into line elements corresponding to portions of airways, on which we can describe the density of aircraft as a function of time and of the coordinate along the line. Such an approach focuses on the conservation of aircraft on the line elements. A traditional way to describe the evolution of the density along these portions of lines is to use a *partial differential equation* (PDE). This PDE appears naturally in highway traffic and is called the Lighthill-Whitham-Richards (LWR) PDE [9], [12]. In this work, we will derive a modified version of the LWR PDE specifically applicable to the *Air Traffic Control* (ATC) problem of interest.

The primary goal of this paper is to show that despite the information loss inherent in any Eulerian model, the aircraft count (which is a crucial ATC metric defined in this paper) is predicted accurately. In [2], our goal is to show that fast numerical analysis tools can be applied efficiently to this problem for simulations purposes, and that adjoint based methods can be adapted for this real-time network control problem. The main difference between ours and previous work using LWR models of air traffic [10] or highway traffic [7], [11], [13] is that we generate an optimization technique (with throughput and maximal density as objective function) using the continuous PDE directly, instead of its discretization. This enables the use of fast numerical techniques specifically developed to treat first order hyperbolic PDEs with discontinuous solutions. Furthermore, the optimization methodology enables the treatment of constraints in the control and the state.

This paper is organized as follows. Since the air traffic flow problem is significantly different from the highway problem, we will first rederive the LWR PDE for the case of interest in Section II, and generalize it to a network. Then, we determine an analytical solution for the case of time-invariant velocity control, which, in [2], will be used for numerical validation purposes. In Section III, we explain how to identify the numerical values of the parameters for the airspace of interest, using *Enhanced Traffic Management System* (ETMS) data. Finally, in Section IV, we validate the model against real data. In [2], we use this framework to describe the NAS, and show how to control it.

II. A new Eulerian network model of airspace

A. A modified LWR model of air traffic

In describing the air traffic system, like the road system, one has to first look at aircraft (or cars) present in the system and estimate a density of vehicles. Therefore, given a portion of airspace (airway or sector), one needs to introduce the *aircraft count* [4] defined as the number of aircraft in that region. Let us consider a portion airway of length L, described by a coordinate $x \in [0, L]$. The number of aircraft in the segment $[0, x]$ at time t is called $n(x, t)$. Thus, $n(L, t)$ represents the aircraft count on the portion of airway $[0, L]$. Assuming a static mean velocity profile v defined on $[0, L]$, $v(x) > 0$ represents the mean velocity of aircraft at location x, and the motion of an aircraft is described by the dynamical system $\dot{x} = v(x)$.

Introducing $K(x) = \int_0^x \frac{ds}{v(s)}$, it is fairly easy to see that if an aircraft were at location x_0 at time t_0, it would be at x at time $t = t_0 + K(x) - K(x_0)$. Because of the sign of v, K is invertible, and therefore x_0 is related to x, t and t_0 by $x_0 = K^{-1}(K(x) - (t - t_0))$.

Consider a point x and $x + h > x$. The number of aircraft between x and $x + h$ at t can be related to the number of aircraft at t_0 at locations $x_0 = K^{-1}(K(x) - (t - t_0))$ and $x_h = K^{-1}(K(x + h) - (t - t_0))$ (conservation of aircraft): $n(x + h, t) - n(x, t) = n(K^{-1}(K(x + h) - (t - t_0)), t_0) - n(K^{-1}(K(x) - (t - t_0)), t_0)$. In other words, assuming that there is no inflow at 0,

$$n(x, t) = n(K^{-1}(K(x) - (t - t_0)), t_0)$$

Some simple algebra (two successive applications of the chain rule) shows that the space derivative and the time derivative of n are related by:

$$\frac{\partial n(x,t)}{\partial t} + v(x)\frac{\partial n(x,t)}{\partial x} = 0$$

We recognize this as a first order linear hyperbolic PDE, and can now enunciate the following proposition:

Proposition 1. *Let $v(\cdot) : [0, L] \to \mathbb{R}^+$ be a $PC_1([0, L])$ function with a finite number of discontinuities at $\{x_k\}_{k\in\{0,\cdots,K\}}$ on $[0, L]$ such that $\exists m > 0$, $m \le v(x)$ for all $x \in [0, l]$. Let $q^{in} \in C_0([0, T])$ and $n_0 \in C_0([0, L])$. Then the following PDE*

$$\begin{cases} \frac{\partial n(x,t)}{\partial t} + v(x)\frac{\partial n(x,t)}{\partial x} = q^{in}(t) & \text{in } [0, L] \times (0, T] \\ n(x, 0) = n_0(x) & \text{in } [0, L] \times \{0\} \\ n(0, t) = 0 & \text{in } \{0\} \times (0, T] \end{cases} \quad (1)$$

admits a unique continuous (weak) solution, given by:

$$\begin{aligned} n(x, t) &= n_0\left(K^{-1}(K(x) - t)\right) + \int_0^t q^{in}(u)du \\ &\qquad \text{if } t \le \int_0^x \tfrac{du}{v(u)} \\ n(x, t) &= \int_{t-K(x)+K(0)}^t q^{in}(u)du \\ &\qquad \text{if } t \ge \int_0^x \tfrac{du}{v(u)} \end{aligned} \quad (2)$$

where $K(x) = \int_0^x \frac{du}{v(u)}$, and K^{-1} is its inverse.

Proof — Existence: K is well defined because $v(x) \ge m$ for all $x \in [0, l]$. Its inverse exists because K is (strictly) increasing. It is easy to check that (2) satisfies (1) almost everywhere, and that it is continuous. This solution has been constructed using a technique analogous to the algorithm of Bayen and Tomlin [3] based on the method of characteristics.

Uniqueness: Let us call n_1 and n_2 two continuous weak solutions of (1). Call $\delta := n_1 - n_2$. δ satisfies: $\frac{\partial \delta}{\partial t} + v(x)\frac{\partial \delta}{\partial x} = 0$ a.e. in $[0, L] \times (0, T]$, $\delta(x, 0) = n_0(x)$ in $[0, L] \times \{0\}$ and $\delta(0, t) = 0$ in $\{0\} \times (0, T]$. Multiplying this PDE by δ and integrating from $x_0 = 0$ to the first discontinuity x_1 of $v(\cdot)$ gives:

$$\int_{x_0}^{x_1} \delta(u,t)\frac{\partial \delta}{\partial t}(u,t)du + \int_{x_0}^{x_1} v(u)\delta(u,t)\frac{\partial \delta}{\partial x}(u,t)du = 0$$

from which we deduce

$$\frac{1}{2}\frac{d}{dt}\int_{x_0}^{x_1} \delta(u,t)^2 du + \int_{x_0}^{x_1} v(u)\delta(u,t)\frac{\partial \delta}{\partial x}(u,t)du = 0$$

Integrating by parts gives

$$\begin{aligned} \frac{1}{2}\frac{d}{dt}\int_{x_0}^{x_1} \delta(u,t)^2 du &\le \int_{x_0}^{x_1} c'(u)\frac{1}{2}\delta(u,t)^2 du - \left[v(u)\frac{1}{2}\delta(u,t)^2\right]_{x_0}^{x_1} \\ &\le \int_{x_0}^{x_1} c'(u)\frac{1}{2}\delta(u,t)^2 du \end{aligned}$$

since $\delta(x_0, t) = 0$ and $v(x_1) > 0$. Using the fact that $v(\cdot) \in C_1([x_0, x_1])$, $\exists M > 0$, $|c'(x)| \le M$ for all $x \in [x_0, x_1]$, from which we deduce

$$\int_{x_0}^{x_1} c'(u)\frac{1}{2}\delta(u,t)^2 du \le M\int_{x_0}^{x_1} \frac{1}{2}\delta(u,t)^2 du$$

then, using Gronwall's lemma,

$$\frac{1}{2}\frac{d}{dt}\int_{x_0}^{x_1} \delta(u,t)^2 du \le M\int_{x_0}^{x_1} \frac{1}{2}\delta(u,t)^2 du$$

which implies $\delta(x, t) = 0$ almost everywhere in $[x_0, x_1]$. By continuity, $n_1(x, t) = n_2(x, t)$ everywhere in $[x_0, x_1]$, and therefore at x_1. The same proof applies to $[x_1, x_2]$ since $n_1(x_1, t) = n_2(x_1, t)$ for all t. By induction on x_k, they are equal everywhere in $[x_0, x_k]$ and therefore in $[0, L]$. □

In equation (1), q^{in} represents the inflow at the entrance of the link (i.e. at $x = 0$). In highway traffic flow analysis, n is sometimes referred to as cumulative flow. It can be related to the vehicle density through the integral relation

$$n(x, t) = \int_0^x \rho(u, t)du \quad (3)$$

where $\rho(x, t)$ is the vehicle density. It can be checked that the vehicle density satisfies the following PDE:

$$\begin{cases} \frac{\partial \rho(x,t)}{\partial t} + \frac{\partial}{\partial x}(\rho(x, t)v(x)) = 0 \\ \rho(0, t)v(0) = q^{\text{in}}(t) \\ \rho(x, 0) = \rho_0(x) \end{cases} \quad (4)$$

Equation (4) can be related to equation (1) by a simple integration of ρ along $[0, x]$. Equation (4) is a mass conservation equation, written in conservation law form. This equation is very closely related to the original LWR PDE [9], [12]. The LWR PDE, originally developed for highways, in fact reads $\frac{\partial \rho(x,t)}{\partial t} + \frac{\partial}{\partial x}(q(\rho(x, t))) = 0$, where $q(\cdot)$ is a flux function depending on ρ, which relates the car density on the highway to the flux. In practice, $q(\cdot)$ is empirically determined, and several models of $q(\cdot)$ are currently used [1], [7], [6]. Computation of the numerical value of the parameters associated with these flux functions is a difficult task, which can for example be achieved with Kalman filtering techniques [13]. In the present case, the flux function

$q(\cdot)$ is replaced by a mean velocity $v(\cdot)$ multiplied by the density. In [2], $v(x)$ will also depend on t and will be the control input of the system. It is also possible to rewrite the first equation in (4) as

$$\frac{\partial \rho(x,t)v(x)}{\partial t} + v(x)\frac{\partial}{\partial x}(\rho(x,t)v(x)) = 0$$

which provides the following corollary:

Corollary 2. *The corresponding solution for ρ is given by:*

$$\rho(x,t) = \begin{cases} \rho(K^{-1}(K(x)-t),0)\frac{v(K^{-1}(K(x)-t))}{v(x)} & \text{if } t \le K(x) \\ \frac{q^{in}(t-K(x))}{v(x)} & \text{otherwise} \end{cases}$$

The interpretation[1] of the corollary is the following: the quantity ρv is conserved along the characteristic curves $t - t_0 = K(x) - K(x_0)$. At this stage, ρ is defined by $\rho = \frac{\partial n}{\partial x}$ and satisfies (4). However, unlike for highway traffic, the density ρ might not be the best way to characterize the flow situation at a given time: if the number of aircraft in the system is small, ρ will be a set of spikes, which is intractable numerically. Therefore, a more tractable quantity to work with would be $\frac{\delta n}{\delta x}$, where δn represents the number of aircraft contained in a finite interval of length δx. This quantity does not a priori satisfy the PDE (4). It is meaningful to introduce an additional "density-like" quantity called r, which satisfies the PDE and for which we can suggest a physical interpretation.

$$r(x,t) = \frac{[n(K^{-1}(K(x)-(t-t_{\text{ref}})))-n(K^{-1}(K(x)-(t+t_{\text{ref}})))]}{2t_{\text{ref}}v(x)}$$

where t_{ref} is a reference time. $r(x,t)v(x)$ represents the number of aircraft included into a window of $2t_{\text{ref}}$ time units of location x and can be referred as "time density". This way of accounting for density is meaningful for Air Traffic Control, since it incorporates a time scale t_{ref} into the density computation and thus provides axess to the time separation between aircraft. It is easy to show that r itself satisfies the same PDE as ρ for any value of t_{ref}:

$$\frac{\partial r(x,t)}{\partial t} + \frac{\partial (r(x,t)v(x))}{\partial x} = 0$$

One can also show that when $t_{\text{ref}} \to 0$, r and ρ are the same:

$$\begin{aligned}\lim_{t_{\text{ref}}\to 0} &\left[\frac{n(K^{-1}(K(x)-(t-t_{\text{ref}})))-n(K^{-1}(K(x)-(t+t_{\text{ref}})))}{2t_{\text{ref}}v(x)}\right] \\ &= \lim_{t_{\text{ref}}\to 0} \frac{n(x,-t_{\text{ref}}) - n(x,t_{\text{ref}})}{2t_{\text{ref}}v(x)} = \frac{1}{v(x)}\left(-\frac{\partial n(x,t)}{\partial t}\right) \\ &= \frac{1}{v(x)}v(x)\frac{\partial n(x,t)}{\partial x} = \rho(x)\end{aligned}$$

At this stage, we have three quantities: ρ, $\frac{\delta n}{\delta x}$ and r. The meaning of ρ as we know it in fluid mechanics assumes a large number of particles (i.e. aircraft) per unit volume (the threshold is defined by the Knüdsen number). In the present case, the number of aircraft we consider will almost certainly be below this number, meaning that the fluid approximation is questionable. This means that instead of using $\rho = \frac{\partial n}{\partial x}$, we will use $\rho \sim \frac{\delta n}{\delta x}$ in the PDE: we will justify this approximation with appropriate validations. In particular, we will have to make a choice of a numerical parameter called $L_{\text{ref}} := \delta x/2$. This will be done in Section III. We then will validate the model against real data to show its accuracy and predictive capabilities (Section IV).

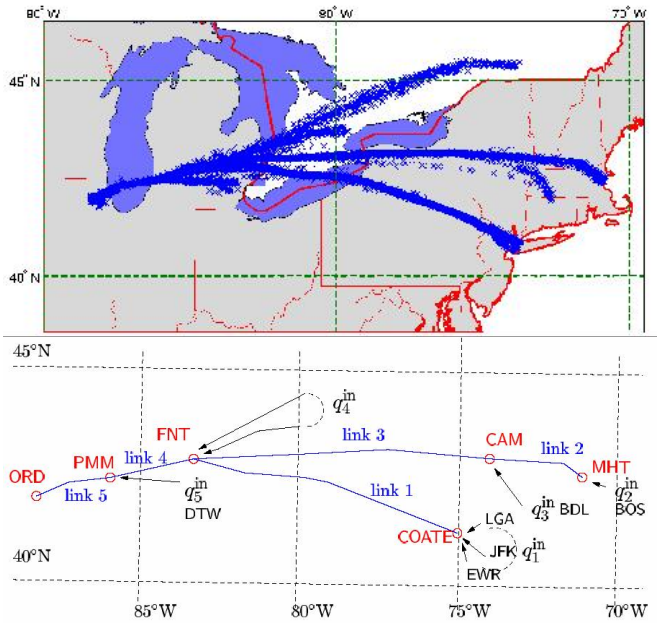

Fig. 1. **Top:** Tracks of flights incoming into Chicago (ORD). The upper stream comes from Canada, the lower from New York and Boston (BOS). Additional streams merge into the network (Detroit and Hartford Bradley). **Bottom:** Network model for the tracks shown above, with waypoints labeled. The model includes five links, merging into ORD. The corresponding inflow terms correspond to a single airport as in BOS or Detroit (DTW), or to a set of airports, as in New York (EWR, JFK, LGA).

B. Network model

The model of the previous section describes traffic on a single portion of airway or line element. As was done earlier for highways [8], this model can be generalized to airway networks, i.e. sets of interconnected airways, as shown in Figure 1 for inbound traffic into Chicago (ORD). We now derive a framework to describe unidirectional air traffic. We describe the topology of the network by a unidirectional graph (E,V), in which E is the set of edges or links, and V the set of vertices. For simplicity of notation, we will index the links by $i \in \{1,\cdots,N\}$, rather than by the indices of the two corresponding vertices. For all $i \in \{1,\cdots,N\}$, we call $\mathcal{U}(i)$ the set of upstream links merging into link i, and $\mathcal{M}$ the set of links for which the upstream links are only merging. The number of links merging into a single link is not limited; it is possible to have $|\mathcal{U}(i)| > 2$. If there is a divergence at the end of a link i, we assume for simplicity that there are only two emanating links from the corresponding vertex. We

[1]Note that a more convenient way to write the solution for $t \le K(x)$ is $\rho(x,t) = \rho(x_0(x,t),0)\frac{v(x_0)}{v(x)}$ where $x_0 = K^{-1}(K(x)-t)$ is the origin of the characteristic curve of the system in the (x,t) plane, going through x at t.

index by i_l and i_r the two emanating links (left and right), and call β_i the portion of the flow going from i to i_l, and $1-\beta_i$ the proportion of the flow going from i to i_r. We call $\mathcal{D}$ the set of links with a divergence at the end of it. The β_i are not known a priori and have to be determined. These coefficients might depend on t as well, and therefore a dependence $\beta_i(t)$ is included in the model.

N	number of links
$\mathcal{S}$	set of source links
$\mathcal{M}$	set of links into which other links merge
$\mathcal{D}$	set of links ending in a fork
$\mathcal{U}(i)$	set of links merging into link i (if $i \in \mathcal{M}$)
i_l, i_r	indices of the two links of a fork if $i \in \mathcal{D}$
L_i	length of link i
x_i	arclength on link i: $x_i \in [0, L_i]$
$\rho_i(x_i, t)$	aircraft density on link i
$\rho_i^\circ(x_i)$	initial aircraft density on link i
$v_i(x_i)$	velocity profile on link i: $v_i(\cdot) : [0, L_i] \to \mathbb{R}^+$
$q_i^{\text{in}}(t)$	inflow at $x_i = 0$ for link i (if applicable)
$\beta_i(t)$	portion of ρ_i which flows into link i_l

TABLE I

NOTATION FOR THE NETWORK PROBLEM.

We call $\mathcal{S}$ the set of sources in the network, and $\mathcal{T}$ a sink of the network, at which we might want to perform optimization. We index all variables of the previous section by i: the aircraft density on link i is ρ_i, the coordinate is x_i, the main velocity profile is v_i, etc. Note that we are NOT using Einstein's notation. The notation is summarized in Table I. The governing PDE system thus reads:

$$\begin{cases} \frac{\partial \rho_i(x_i,t)}{\partial t} + \frac{\partial}{\partial x_i}\left(\rho_i(x_i,t)v_i(x_i)\right) = 0 \\ \qquad\qquad\qquad\qquad\qquad\qquad \forall i \in \{1,\cdots,N\} \\ \rho_i(x,0) = \rho_i^\circ(x) \qquad\qquad \forall i \in \{1,\cdots,N\} \\ \rho_i(0,t)v_i(0,t) = \sum_{j\in\mathcal{U}(i)} \rho_j(L_j,t)v_j(L_j,t) + q_i^{\text{in}}(t) \\ \qquad\qquad\qquad\qquad\qquad\qquad \forall i \in \mathcal{M} \\ \begin{cases} \rho_{i_l}(0,t)v_{i_l}(0,t) = \beta_i(t)\,\rho_i(L_i,t)v_i(L_i,t) \\ \rho_{i_r}(0,t)v_{i_r}(0,t) = (1-\beta_i(t))\rho_i(L_i,t)v_i(L_i,t) \end{cases} \\ \qquad\qquad\qquad\qquad\qquad\qquad \forall i \in \mathcal{D} \\ \rho_i(0,t)v_i(0,t) = q_i^{\text{in}}(t) \qquad\qquad \forall i \in \mathcal{S} \end{cases} \tag{5}$$

In the previous system, the PDE (first equation) describes the evolution of ρ_i on each link. The second equation is the initial condition (i.e. the initial density of aircraft on each link). The third equation expresses the conservation of aircraft at the merging points. The fourth and fifth equation express the conservation of aircraft at the divergence points. The last equation expresses the boundary conditions (inflow at the sources of the network). The sinks of the system are free boundary conditions, and therefore do not appear in the previous system. Assuming one can solve (5), it is possible to use the solution to compute (and optimize) certain metrics useful for ATC. For example, one quantity of interest is aircraft count, which is the number of aircraft in a given sector. If all links of a given sector are indexed by $i \in$ Sec, the aircraft count of the sector is obtained by $\sum_{i\in\text{Sec}} \int_0^{L_i} \rho_i(x_i,t)dx_i$.

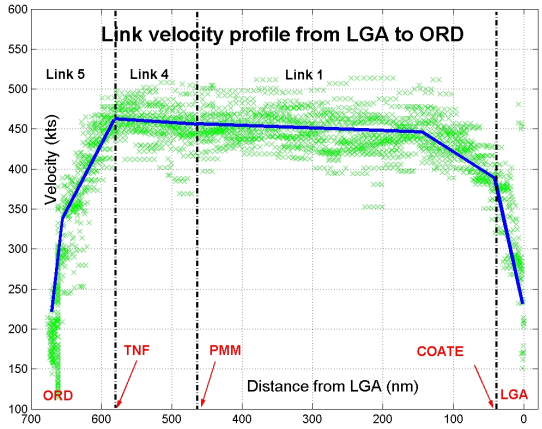

Fig. 2. Example of velocity profile used for the junction LGA-ORD. The horizontal coordinate is the distance from ORD in nm. The corresponding links are shown as well as the location of the airspace fixes between the links. The curve is a piecewise affine fit obtained using least squares.

III. Application to Air Traffic Flow

In this section, we first explain how to identify the mean velocity profiles from real air traffic data. We then explain how to choose the numerical value of parameters of the model. In the next section, these choices will be validated against real data.

A. System identification: main velocity profiles

We first explain how we identify the mean velocity profiles $v_i(x_i)$ on each link. We use *Enhanced Traffic Management System* (ETMS) data, which we can obtain at NASA Ames (see [4] for a description of ETMS data). From ETMS data, we can obtain useful flight information at a 1 minute rate: position of each aircraft in the NAS, altitude, velocity, flight plan (i.e. set of airways and wayoints). From this data, we are able to identify the routes in which traffic is concentrated. Note that in recent work, Menon et al. [10] focused on creating a tool which performs similar tasks automatically at a NAS-wide level, using FACET [4], a tool developed by NASA Ames. The details of this tool are not available to us, and we developed our own method to identify the main links used by aircraft in the NAS. We analyze 24 hours of ETMS data and select all aircraft using the links of the network shown in Figure 1. We identify all aircraft which use each of the links, and record all tracks and corresponding speeds between takeoff and landing. For each of the links shown in Figure 1, we identify the mean velocity profiles as piecewise affine function, using a least squares fit. The total number of aircraft used is 220. The result for the flight New York – Chicago is displayed in Figure 2. As can be seen, once the En Route altitude is reached, the curve fits are almost flat, which means that the aircraft are En Route at a high altitude cruise speed. It can also be seen from Figure 2 that the data is relatively broadly spread (standard deviation 19.6 kts). This suggests deriving multilayer models: dividing the

link in sublayers corresponding to altitudes (with different speed profiles) has the benefit of being more precise, as aircraft tend to have a Mach number – and therefore speed which is a function of altitude. This will be considered in the future.

B. Initial and boundary conditions

Once the mean velocity profiles are computed, we identify the initial density of aircraft and the inflow (boundary conditions) in the network. The initial position of the aircraft is easy to extract from the ETMS data: at the prescribed time, all airborne aircraft which are on the relevant links are selected.

1) For any selected aircraft a at location x_i^a on link i, the classical density $\rho_i(x_i,0) = \rho_i^\circ(x_i)$ is taken to be a "box" around x_i^a, of length $2L_{\text{ref}}$. Calling χ_I the characteristic function of an interval I (i.e. equal to 0 outside of I and 1 inside), $\rho_i(x_i,0)$ is $\frac{1}{2L_{\text{ref}}}\chi_{[x_i^a-L_{\text{ref}},x_i^a+L_{\text{ref}}]}(x_i)$. Taking all aircraft initially airborne on link i, the density is: $\rho_i^\circ(x_i) = \sum_{a \text{ in link } i} \frac{1}{2L_{\text{ref}}}\chi_{[x_i^a-L_{\text{ref}},x_i^a+L_{\text{ref}}]}(x_i)$

2) Similarly, the density-like function r is computed using the knowledge of the mean velocity profile along link i, called $v_i(x_i)$, and the parameter t_{ref}: $r_i^\circ(x_i) =$

$\sum_{a \text{ in link } i} \frac{1}{2t_{\text{ref}}v_i(x_i^a)}\chi_{[x_i^a-t_{\text{ref}}v_i(x_i^a),x_i^a+t_{\text{ref}}v_i(x_i^a)]}(x_i)$

The inflows (boundary conditions) can also be extracted from ETMS data: each time an aircraft takes off, it will appear in the ETMS data as soon as it is airborne. The ETMS data also shows the filed flight plan, which we select when it intends to use the links of interest to us. $q^{\text{in}}(t)$ is computed the following way. At any instant when the data shows a new aircraft on one of the source links $\mathcal{S}$, the track is in general passed the entrance point of that link (because of the sampling rate of 3 minutes). Calling x_i^a the position of this aircraft on link i at the first time it appears, we compute the time t_a at which it crossed the location $x_i = 0$ (using the knowledge of the mean velocity profile on the link). We then use one of the two definitions above to compute $q^{\text{in}}(t)$ corresponding to either ρ or r.

C. Identifying the numerical parameters

As explained in Section III-B, we have two ways of describing the density of aircraft in the network, in terms of a density function ρ and a "density-like" function r, which respectively account for spatial and temporal distribution of aircraft. The function ρ depends on the numerical parameter L_{ref}, which we need to adjust. The value of this parameter is crucial for predicting aircraft count: Figure 3 shows how errors can occur in translating density functions into aircraft count. We want to determine the choice of parameters leading to the smallest error in aircraft count prediction.

We first run the following set of experiments. For the link New York – Chicago, we run a set of simulations involving N_{aircraft} aircraft, where N_{aircraft} successively takes all values between 1 and 50. We vary L_{ref} between 0 and 120 nm. For each value of N_{aircraft} and L_{ref}, we run 400 experiments. Each experiment corresponds to a uniformly distributed random density of N_{aircraft} aircraft along link 1 in $[0, 400]$ (see Figure 1). The simulation starts at a time t_0 with the density ρ_i° computed as in the previous section, and computes the solution of the LWR PDE until the time $t_0 + \Delta T$. For the experiments, ΔT was chosen equal to one hour (note that the duration of the total flight is on the order of two and a half hours). This solution is compared with the solution obtained by propagating the Lagrangian trajectories of each of the aircraft independently from t_0 to $t_0 + \Delta T$ and computing the resulting density. In mathematical terms, we compare the two following quantities

1) $\rho_i(\cdot, t_0 + \Delta T)$ computed by the LWR PDE (5)

2) $\tilde{\rho}_i(\cdot, t_0 + \Delta T) :=$

$\sum_{a \text{ in link } i} \frac{1}{2L_{\text{ref}}}\chi_{[x_i^a(t_0+\Delta T)-L_{\text{ref}},x_i^a(t_0+\Delta T)+L_{\text{ref}}]}(\cdot)$ where $x_i^a(t_0 + \Delta T)$ is the position of aircraft a at time $t_0 + \Delta T$.

In order to characterize the best choice of numerical parameters, we compute the following two quantities (notations refer to Figure 1):

1) The relative density error, defined by

$$\frac{\sum_{i=1,4,5} \int_0^{L_i} |\rho_i(x_i, t_0 + \Delta T) - \tilde{\rho}_i(x_i, t_0 + \Delta T)|\, dx_i}{\sum_{i=1,4,5} \int_0^{L_i} \rho_i(x_i, t_0 + \Delta T) dx_i}$$

This quantity represents the error in density prediction due to the propagation of ρ by the PDE.

2) The absolute aircraft count error, defined by

$$\sum_{i=1,4,5} \sum_{\text{sublinks of } i} \left| \int_0^{L_i} \rho_i(x_i, t_0 + \Delta T) dx_i - \sharp(a | a \in \text{link } i) \right|$$

where $\sharp$ means number. This quantity is the sum of count error for all sublinks of links 1,4, and 5. Typically, a link is divided into sublinks which correspond to different airspace sectors. For example, if link 1 goes through 8 sectors, we divide it in 8 sublinks and are interested in the aircraft counts on these sublinks. This error thus estimates the difference between the number of aircraft predicted by the PDE and the number obtained by a Lagrangian propagation of aircraft, where the error is the sum of all errors on the sublinks.

The computation of both quantities is illustrated in Figure 4. The relative density error and absolute aircraft count error are averaged (over the 400 runs) and plotted for the range of n and L_{ref} considered. The result is shown in Figure 5. The left plot shows the relative density error. As expected, the error decreases when the number of aircraft increases and L_{ref} increases (typically in fluid mechanics, the Knüdsen number defines the number of particles per volume above which the fluid approximation becomes valid). The right plot shows the

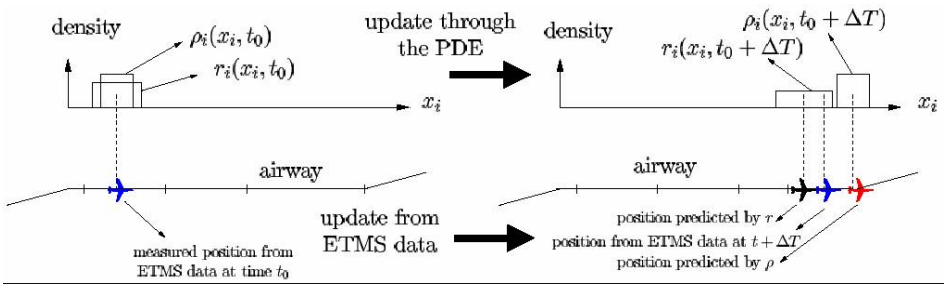

Fig. 3. Different predictions obtained by the use of ρ and r for aircraft density. Above: density propagation through the PDE system (5); below: position update from ETMS data and from the PDE.

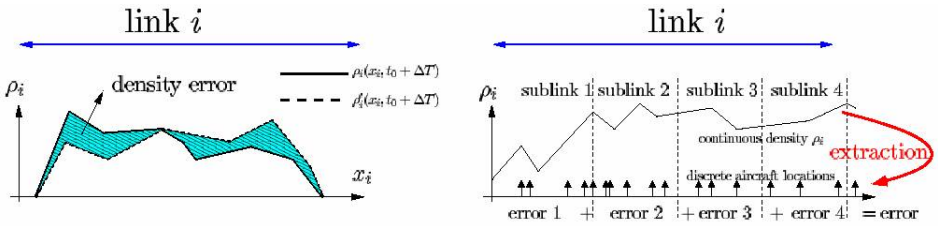

Fig. 4. **Left:** Illustration of the computation of the relative density error depicted in Figure 5. The difference between the two density curves (shaded area) is divided by the area below the ρ_i curve. **Right:** Illustration of the computation of the error in aircraft count. The link is divided into sublinks (which can correspond to sectors). For each of these sublinks, we compare the number of aircraft predicted by the method (depicted by arrows, which are computed from the density) with the number of aircraft obtained by a Lagrangian propagation of the trajectories. The error is the sum of errors for all sublinks, i.e. the sum of the errors in sector counts.

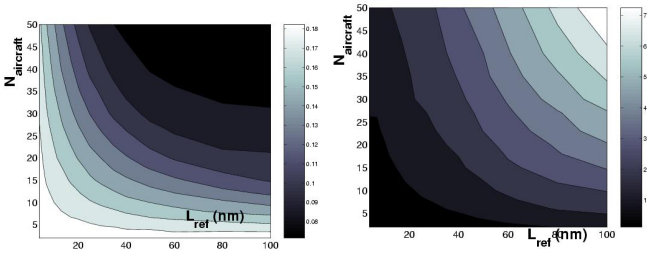

Fig. 5. **Top:** Relative density error between the density predicted by the Eulerian PDE propagation of the density. **Bottom:** Absolute aircraft count error for the junction New York – Chicago.

absolute aircraft count error, averaged over 400 simulations. For this plot, each of the links 1, 4 and 5 have been divided in sublinks (20 total), of about 50 nm length. This is a worst case scneario, i.e. the number of relevant sectors for a flight of this length is never higher. One can see that for $L_{\text{ref}} \leq 60$ and $N_{\text{aircraft}} \geq 25$, the average aircraft count error is always extremely small.

The best choice for L_{ref} is thus obtained at the intersection of the lowest level sets of both plots of Figure 5, i.e. for a range of $L_{\text{ref}} \in [20, 60]$ and $N_{\text{aircraft}} \geq 20$.

IV. Validation of the Model

In the previous section, we have shown that the use of the modified LWR PDE either with r (with any t_{ref}) or $\rho \sim \frac{\delta n}{\delta x}$ (with an appropriate choice of L_{ref}) enables accurate aircraft count predictions. In this section, we validate the model against real data: in particular, we had made the assumption that $v_i(x_i, t) = v_i(x_i)$. As we know, this will not be the case in general. Therefore we run simulations and assess if the model is still in agreement with real data over two separate experiments.

A. Static validation

In the first experiment, we use the static velocity profiles $v_i(\cdot)$ determined in the previous sections for the validation of the method. We use a 6 hour ETMS data set. From this data set, we extract the position of the aircraft, at the initial time, construct the corresponding initial aircraft density, and propagate it through the PDE system. At any given time, we compare the aircraft count predicted by our method and the aircraft count provided by the ETMS data (which is exact, since it provides the position of each aircraft). We compute the error in aircraft count for a set of ten sublinks for the network shown in Figure 1. The result is shown in Figure 6 (left). The window width L_{ref} was taken equal to 15 nm. One can see on the left plot that the total error (for all airborne aircraft in this airspace) is relatively low (the maximal error is 7 aircraft). In fact, the results are much better than they seem: most of the errors come from the fact that the aircraft distribution is such that there is always at least one or two aircraft close to a sublink boundary, which will thus be counted in the wrong sublink. In fact, this is not really a problem, as it is more an artifact of the computation rather than a true error (Figure 7 shows that the density unambiguously shows where the aircraft is). Furthermore, some of the errors in aircraft count are due to errors present in the ETMS data (some have clearly erroneous data; this fact has also been reported in [5]).

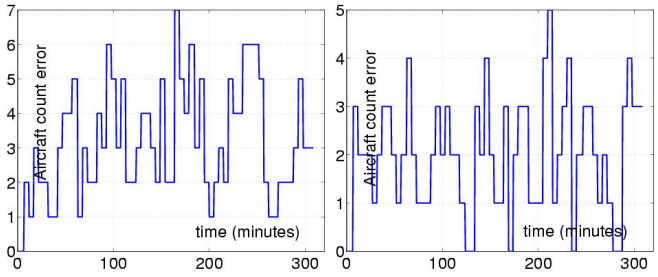

Fig. 6. **Left:** Error in aircraft count for the static validation over a five hour period. **Right:** Error in aircraft count for the dynamic validation over a five hour period.

B. Dynamic validation

We extend the validation to a case in which the velocity profiles are time dependent, i.e. $v_i(x_i, t)$. The details of the identification of these profiles are technical and are not explained here. The comparison is the same as in the static case. Note that our analytical solution does not handle dynamic velocities. This difficulty is alleviated by using a numerical scheme presented in the companion paper [2]. The results are shown in Figure 6 and are more accurate than the static results, as expected. The same remarks apply, and the results are again affected by the quality of ETMS data and the inclusion of the computation artifact. The only weakness of this validation is that the simulation is run using data from the same day as the data used in identification. A way to improve this would be to perform the velocity identification with data of a given day over a 24 hour period, and validate it over the next 24 hour period, using the fact that there is periodicity in the traffic for normal days. This was not done here due to lack of available data. An animation (.avi movie file) corresponding to the snapshots of Figure 6 is available at [14].

In both cases, the validation is very encouraging and shows strong predictive capability for our model. The model was also tested successfully using data from the western states (Oakland Center with traffic incoming into Bay Area airports), though for brevity these results are not included here. Finally, in [2], we will use the model for control: in that case, one of the control variables is speed, which means that we will have direct access to $v_i(x_i, t)$ (since we compute it). This alleviates difficulties of mean velocity profile identification shown before.

Acknowledgments

We are grateful to Dr. P.K. Menon for conversations which inspired this work, Dr. Gano Chatterji for his ongoing support and suggestions which went into modeling this work, and to Dr. George Meyer for his support in this project. We are thankful to Pr. Tom Bewley for useful conversations regarding the application of the adjoint method to flow control, and his help in the original formulation of the control problem. Pr. Tai-Pin Liu helped define the PDE used for this model.

REFERENCES

[1] R. ANSORGE. What does the entropy condition mean in traffic flow theory? *Transportation Research*, 24B(2):133–143, 1990.

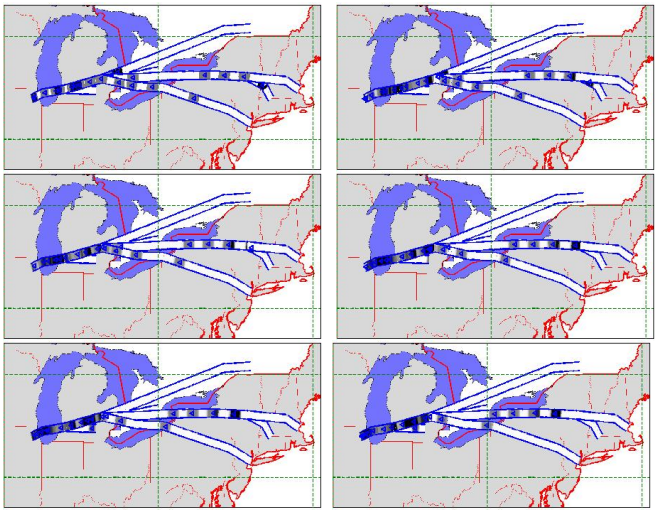

Fig. 7. Display of the traffic situation for the static validation. The density of the links is depicted by the color. The colored rectangles shown in this plot represent the density. The colorscale is: white for zero density; black for highest density. The actual aircraft positions are superimposed (triangles). Traffic is shown at t_0 (top left), $t_0 + 8\,\mathrm{min}$ (top right), $t_0 + 16\,\mathrm{min}$ (middle left), etc. As can be seen, the peaks of density corresponds to the actual positions of the aircraft.

[2] A. M. BAYEN, R. RAFFARD, and C. J. TOMLIN. Adjoint-based constrained control of Eulerian transportation networks: application to Air Traffic Control. In *Proceedings of the American Control Conference*, Boston, June 2004.

[3] A. M. BAYEN and C. J. TOMLIN. A construction procedure using characteristics for viscosity solutions of the Hamilton-Jacobi equation. In *Proceedings of the* 40^{th} *IEEE Conference on Decision and Control*, pages 1657–1662, Orlando, Dec. 2001.

[4] K. BILIMORIA, B. SRIDHAR, G. CHATTERJI, K. SETH, and S.GRAABE. FACET: Future ATM Concepts Evaluation Tool. In *Proceedings of the 3rd USA/Europe Air Traffic Management R&D Seminar*, Naples, Italy, June 2001.

[5] G. CHATTERJI, B. SRIDHAR, and D. KIM. Analysis of ETMS data qualiy for traffic flow management decisions. In *Proceedings of the AIAA Conference on Guidance, Navigation and Control*, Austin, TX, Aug. 2003. Paper 2003-5626.

[6] C. CHEN, Z. JIA, and P. VARAIYA. Causes and cures of highway congestion. *IEEE Control Systems Magazine*, 21(4):26–33, 2001.

[7] C. DAGANZO. The cell transmission model: a dynamic representation of highway traffic consistent with the hydrodynamic theory. *Transportation Research*, 28B(4):269–287, 1994.

[8] C. DAGANZO. The cell transmission model, part II: network traffic. *Transportation Research*, 29B(2):79–93, 1995.

[9] M. J. LIGHTHILL and G. B. WHITHAM. On kinematic waves. II. A theory of traffic flow on long crowded roads. *Proceedings of the Royal Society of London*, 229(1178):317–345, 1956.

[10] P. K. MENON, G. D. SWERIDUK, and K. BILIMORIA. A new approach for modeling, analysis and control of air traffic flow. In *Proceedings of the AIAA Conference on Guidance, Navigation and Control*, Monterey, CA, Aug. 2002. Paper 2002-5012.

[11] L. MUNOZ, X. SUN, R. HOROWITZ, and L. ALVAREZ. Traffic density estimation with the cell transmission model. In *Proceedings of the American Control Conference*, Denver, CO, June 2003.

[12] P. I. RICHARDS. Shock waves on the highway. *Operations Research*, 4(1):42–51, 1956.

[13] Y. WANG, M. PAPAGEORGIOU, and A. MESSMER. Motorway traffic state estimation based on extended Kalman filter. In *Proceedings of the European Control Conference*, Cambridge, U.K., Sep. 2003.

[14] `http://cherokee.stanford.edu/~bayen/ACC04.html`.